JACS
JOURNAL OF THE AMERICAN CHEMICAL SOCIETY

Article

pubs.acs.org/JACS

Hepatocyte-Targeting Single Galactose-Appended Naphthalimide: A Tool for Intracellular Thiol Imaging in Vivo

Min Hee Lee,[†] Ji Hye Han,[‡] Pil-Seung Kwon,[§] Sankarprasad Bhuniya,[†] Jin Young Kim,[‡] Jonathan L. Sessler,[∥,⊥] Chulhun Kang,*[,‡] and Jong Seung Kim*[,†]

[†]Department of Chemistry, Korea University, Seoul, 136-701, Korea

[‡]The School of East-West Medical Science, Kyung Hee University, Yongin, 446-701, Korea

[§]Department of Clinical Laboratory Science, Wonkwang Health Science University, Iksan, 570-750, Korea

[∥]Department of Chemistry and Biochemistry, The University of Texas at Austin, Austin, Texas 78712-0165, United States

[⊥]Department of Chemistry, Yonsei University, 262 Seonsanno Sinchon-dong, Seodaemun-gu, Seoul 120-749, Korea

Supporting Information

ABSTRACT: We present the design, synthesis, spectroscopic properties, and biological evaluation of a single galactose-appended naphthalimide (**1**). Probe **1** is a multifunctional molecule that incorporates a thiol-specific cleavable disulfide bond, a masked phthalamide fluorophore, and a single galactose moiety as a hepatocyte-targeting unit. It constitutes a new type of targetable ligand for hepatic thiol imaging in living cells and animals. Confocal microscopic imaging experiments reveal that **1**, but not the galactose-free control system **2**, is preferentially taken up by HepG2 cells through galactose-targeted, ASGP-R-mediated endocytosis. Probe **1** displays a fluorescence emission feature at 540 nm that is induced by exposure to free endogenous thiols, most notably GSH. The liver-specificity of **1** was confirmed in vivo via use of a rat model. The potential utility of this probe in indicating pathogenic states and as a possible screening tool for agents that can manipulate oxidative stress was demonstrated in experiments wherein palmitate was used to induce lipotoxicity in HepG2 cells.

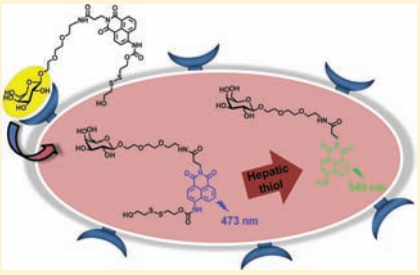

INTRODUCTION

Sensor systems that might allow for the effective, rapid prescreening of drug candidates constitute a major current focus in supramolecular and medicinal chemistry.[1] One important approach involves the development of specific probes that can be used to detect particular cellular components that are associated with disease states in vitro, because ultimately these probes could be used to test quickly the effect, if any, of putative therapeutic agents. However, in contrast to approaches based on screening the structural nature of molecular entities obtained through high-throughput synthesis (e.g., their level of chirality), the cellular probe strategy requires the synthesis of agents that can operate in vitro and perhaps in vivo with high specificity. They also need to provide a read-out that can be monitored readily under the conditions typical of cellular analysis. This makes fluorescent probes of particular interest. While a number of such probes have been put forward for the detection of various cellular components,[2] there remains a need for systems that allow for the detection of metabolites associated with pathogenic cells and whose concentration can be manipulated via the application of external agents (e.g., drug candidates). Among the most important of these metabolites are so-called reduced thiol entities, such as glutathione (GSH), thioredoxin (Trx), cysteine (Cys), and homocysteine (Hcy). These agents, of which GSH is the most abundant (at least in its free, reduced form), play a critical role in maintaining the oxidation−reduction (redox) state of the cell and are the ultimate source of reducing equivalents for enzymes that act to remove reactive oxygen species (ROS), such as catalase, superoxide, dismutase, and glutathione peroxidase.[3] Imbalance of GSH/GSSG ratios in cells is associated with oxidative stress, which, in turn, is directly linked with various diseases including cancer, Parkinson's disease, Alzheimer disease, etc.[4] Conversely, synthetic agents, such as texaphyrins, that exploit GSH-derived reducing equivalents for the tumor-selective production of ROS have attracted attention as experimental drugs.[5] This makes the development of GSH-specific probes of interest; not only could they prove useful in the detection of disease states, they may allow for an early, screening-type analysis of new potential therapeutic agents.

Currently, a number of probes are known that allow for the GSH/GSSG cellular ratios to be estimated.[6] However, these systems operate in a nonspecific manner and do not allow for specific analysis at the level of individual organs. Here, we report a hepatocyte targeting fluorescent probe (**1**) that allows for the real-time fluorescence imaging of reduced thiols both in vitro and in vivo in liver cells. As detailed below, this new probe contains a single galactose subunit and a disulfide-linked naphthalimide.

Received: October 26, 2011
Published: December 15, 2011

   dx.doi.org/10.1021/ja210065g | J. Am. Chem.Soc. 2012, 134, 1316−1322

The galactose subunit serves to guide the probe to hepatocytes, while the disulfide-linked naphthalimide moiety provides for an easy-to-monitor fluorescent change when exposed to endogenous thiols as the result of disulfide cleavage.

We view the liver as the most important target organ for reduced thiol probes. It provides GSH to the bloodstream and other organs, such as the kidneys, lungs, and intestines, and thus plays a critical role in maintaining organismal redox balance.[3,4,7] Moreover, liver-dependent intertissue flow of GSH plays an important role in cancer metastasis at remote sites.[8] Therefore, we view an ability to effect GSH/GSSG detection effectively in the liver as crucial for the development of agents that will allow for the early diagnosis of metastatic cancer, as well as for the screening of drug candidates that might display antineoplastic activity.

RESULTS AND DISCUSSION

Our approach to developing a reduced thiol-specific probe relies on the use of a specific receptor-mediated endocytosis strategy.[9] It exploits the fact that the asialoglycoprotein receptor (ASGP-R) is uniquely expressed on the plasma membrane of mammalian hepatocytes and functions to engender the rapid removal of desialylated glycoproteins from circulation via receptor-mediated endocytosis.[10] It is known that ASGP-R recognizes selectively terminal galactose residues on desialylated glycoproteins, allowing for the selective internalization of the latter species within the hepatocyte. Because of its predominant expression on hepatocytes, its recognized high specificity, and its important role in mediating receptor-mediated endocytosis, ASGP-R has been explored as a means of effecting drug and gene delivery to the liver.[11] In fact, a number of synthetic galactose-terminated ligands have been widely developed as hepatocyte guiding devices.[12−14] Most of these efforts have centered on the use of systems containing multiple galactose residues.[12−15] However, for a small molecule probe, such as what we envision for the recognition of reduced thiols, a single galactose subunit should suffice to achieve recognition and uptake. The development of an effective fluorescent probe for GSH would allow inter alia this postulate to be refuted or confirmed.

Our approach to a liver-specific reduced thiol probe is illustrated in Scheme 1. It involves the linked system **1** that, we suggest, will be selectively recognized by hepatocytes via ASGP-R-mediated endocytosis. Once in the cell, the disulfide bond is expected to undergo disulfide cleavage via reaction with the targeted intracellular thiols. This will release the naphthalimide moiety and lead to easy-to-monitor fluorescence changes. The 4-amino-1,8-naphthalimide is well recognized as a useful fluorescent response element due to its excellent spectroscopic characteristics, including outstanding internal charge transfer (ICT) efficiency, emission at long wavelengths (λ_{max} 540−550 nm) with a high quantum yield. The naphthalimide core is also easily accessible from a synthetic point of view and has structural flexibility that allows for various modifications.[16]

The presumed hepatocyte-targeting probe (**1**) was prepared in accord with the synthetic route outlined in Scheme 2. The naphthalimide derivatives **3a**,**b** and **4a**,**b**[17,18] and the galactose tetraacetate terminated amine (**AcGal-NH$_2$**)[19] were synthesized by adapting procedures reported previously. For the synthesis of **5**, **4a** was reacted with **AcGal-NH$_2$** in the presence of EDCI/DMAP in DMF. Compound **5** was then reacted with triphosgene, followed by treatment with 2,2′-dithiolethanol, to afford **6**. Finally, **1** was obtained by subjecting **6** to deacetetylation in the presence of NaOMe/MeOH. To demonstrate the presumed liver targeting role of the galactose unit in **1**, a structural analogue without galactose, probe **2**, was also prepared. The overall chemical structures of **1** and **2** were confirmed by ^{1}H NMR, ^{13}C NMR, FT-IR, ESI−MS, and HRMS (Supporting Information).

Scheme 1. Schematic Representation of Hepatocyte-Targeted Imaging of 1 through ASGP-R-Mediated Endocytosis to Hepatocytes and Cleavage of the Disulfide Bond To Induce Fluorescence Changes

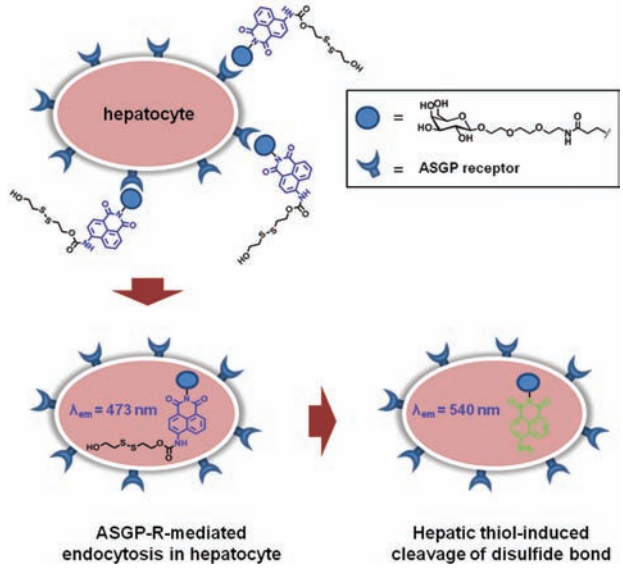

Scheme 2. Synthesis of Probes 1 and 2

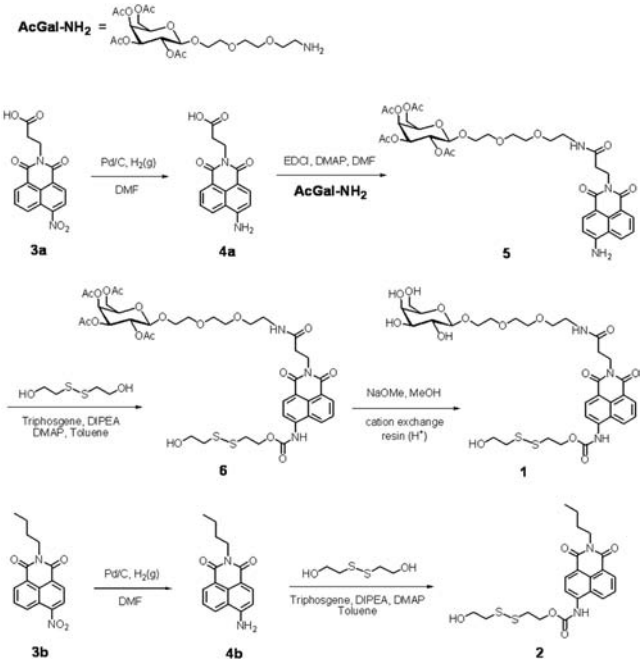

Initial spectroscopic studies of **1** were undertaken by monitoring the changes in the UV/vis and fluorescence spectra seen upon the addition of GSH under physiological conditions (PBS buffer, pH 7.4, 37 °C). In the absence of GSH, probe **1** displays a broad absorption band and a weak emission feature centered around 367 nm ($\varepsilon = 1.6 \times 10^4$ M^{-1} cm^{-1}) and 473 nm ($\Phi_f = 0.29$), respectively. This corresponds to a rather large

dx.doi.org/10.1021/ja210065g | J. Am. Chem.Soc. 2012, 134, 1316−1322

Stokes shift ($\Delta\lambda$ = 106 nm) that is attributed to the fact that **1** contains both electron donor and electron acceptor components and is characterized by strong ICT character (Figure S1). Probe **2** also shows similar photophysical properties (λ_{abs} = 379 nm, $\varepsilon = 2.3 \times 10^4$ M^{-1} cm^{-1}; λ_{em} = 470 nm, Φ_f = 0.15) in MeOH/PBS buffer (v/v, 1:10), pH 7.4 at 37 °C.

As shown in Figure 1a, the addition of GSH (5.0 mM) to a solution of **1** leads to an increase in the fluorescence intensity

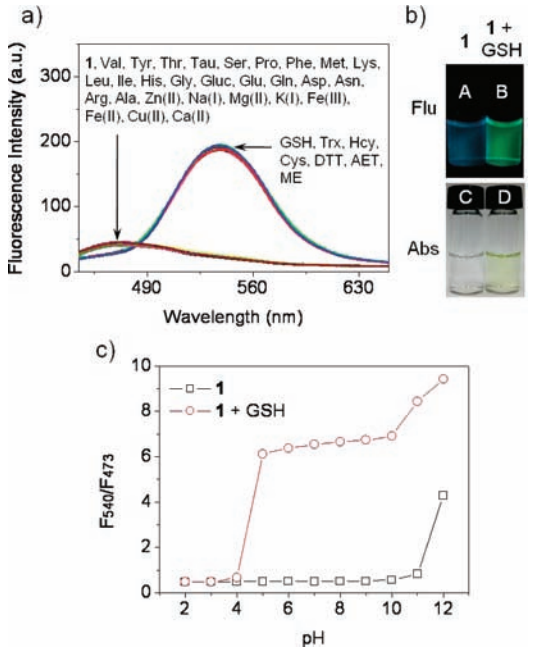

Figure 1. (a) Fluorescence response of **1** (1.0 μM) toward GSH, Cys, Hcy, DTT, AET, MET (5.0 mM, respectively), Trx (5.0 μM), other nonthiol amino acids (5.0 mM, respectively) and metal ions (1.0 mM, respectively). Each spectrum was acquired 1 h after exposure (3 h in the case of GSH) to the analytes in question at 37 °C in PBS buffer (pH 7.4) with λ_{ex} = 428 nm. (b) Fluorescence and color photographs of **1** in the absence (A and C) and presence (B and D) of GSH. (c) The ratio of fluorescence intensity at 540 nm to that at 473 nm (F_{540}/F_{473}) of **1** (1.0 μM) with and without GSH (5.0 mM) as a function of pH. Each point was acquired 3 h after exposure (in the case of GSH) at 37 °C with λ_{ex} = 428 nm.

with a considerable red-shift in the maximum wavelengths of both the absorption and the fluorescence spectra (see also Figure S2). The respective bands appear at 428 ($\Delta\lambda_{abs}$ = 61 nm, $\varepsilon = 1.2 \times 10^4$ M^{-1} cm^{-1}) and 540 nm ($\Delta\lambda_{em}$ = 67 nm, Φ_f = 0.03). Similar spectroscopic changes are also seen upon the addition of various other free thiols, including Trx, Cys, Hcy, 2-aminoethanthiol (AET), 2-mercaptoethanol (ME), and dithiothreitol (DTT). However, such spectral changes were not observed upon exposure to either nonthiol amino acids or biologically essential metal ions (Figure 1a). In the case of GSH, an easy-to-discern color change is seen (Figure 1b).

The pH dependence of the thiol-mediated disulfide bond cleavage step was also investigated. As seen in Figure 1c, probe **1** is stable within the pH range of 2−10. On the other hand, it readily reacts with GSH within the biologically relevant pH range (5−10). Such findings led us to consider that **1** could be used to detect the presence of cellular thiols without interference from pH effects.

Efforts were made to probe the nature of the thiol-induced response. Toward this end, the fluorescence changes seen for probe **1** in the presence of 5.0 mM of GSH were monitored as a function of time (Figure 2a and b). Upon the addition of

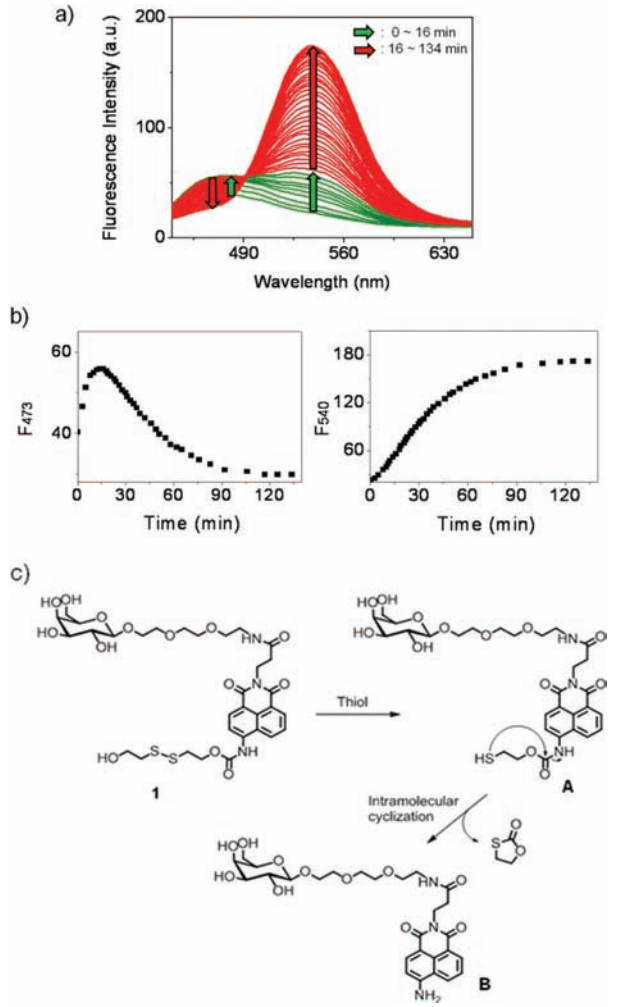

Figure 2. (a) Time-dependent fluorescence spectral changes observed when probe **1** (1.0 μM) was treated with GSH (5.0 mM) at 37 °C in PBS buffer (pH 7.4) with λ_{ex} = 428 nm. (b) Fluorescence intensity changes at 473 nm (F_{473}) and 540 nm (F_{540}) recorded as a function of time. (c) Proposed mechanism corresponding to the reaction of probe **1** with thiol.

GSH to a solution of **1**, the emission intensity at 473 nm was seen to increase initially while a new emission feature was seen at 540 nm (green arrow). These changes take place over the course of 16 min under these experimental conditions. Subsequently, the emission at 473 nm was seen to decrease gradually, while the emission at 540 nm increases (red arrow). The changes occur with an obvious isosbestic point at 492 nm. Within 100 min, the fluorescence intensity reaches a plateau. Similar results were also observed upon the addition of Cys to a solution of **1** (Figure S3).

The biphasic nature of the above changes is consistent with the presence of an intermediate prior to formation of the final product(s). We assign this intermediate to compound **A**, a species that should be formed readily as the result of disulfide cleavage. The formation of this putative intermediate is then followed by slow intramolecular cyclization and cleavage of a neighboring carbamate bond to give aminonaphthalimide (**B**) (Figure 2c). To provide support for this suggestion, the

dx.doi.org/10.1021/ja210065g | J. Am. Chem.Soc. 2012, 134, 1316−1322

products from the reaction of **1** with thiols, MALDI-TOF MS spectroscopic analyses were carried out. Mass peaks at m/z 600.2 and 616.2 corresponding to $[\mathbf{B} + Na^+]$ and $[\mathbf{B} + K^+]$ are clearly observed (Figure S6).

The fluorescence spectral changes seen when probe **1** was treated with increasing quantities of [GSH] (0−1.0 mM) under physiological conditions (PBS buffer, pH 7.4, 37 °C) are shown in Figure S4. The ratio of fluorescence intensities (F_{540}/F_{473}) increases by approximately 10-fold (from 0.7 to 6.7, Figure S4a) with a good linearity with respect to [GSH] being seen over a wide concentration range (0−0.05 mM) (R = 0.99, Figure S4b). From these findings, we infer that probe **1** displays readily detectable changes in its fluorescence signature at micromolar concentrations of thiol level under physiological conditions.

Next, we investigated whether **1** reacts with cellular proteins (thiolated or otherwise) and whether such presumed reactions would lead to fluorescence changes that would interfere with the response produced by free thiols. With this goal in mind, proteins (>10 kDa) from cytosolic cell extracts were dialyzed and then dissolved in PBS buffer. Although discernible fluorescence changes were seen when probe **1** was treated with the protein mixture prepared in this way, much greater changes were observed in the presence of GSH (Figure S5). Because these latter enhancements were seen even in the presence of the protein mixture, we conclude that proteins per se will not preclude the use of probe **1** in vitro or in vivo.

To confirm the presumed target specificity of the galactose-appended probe **1** toward hepatocytes, compounds **1** and **2** were separately incubated with various cells, including HepG2, C2C12, HaCat, and N2a. As can be seen from an inspection of Figure 3, compound **2** displays a strong fluorescence signature

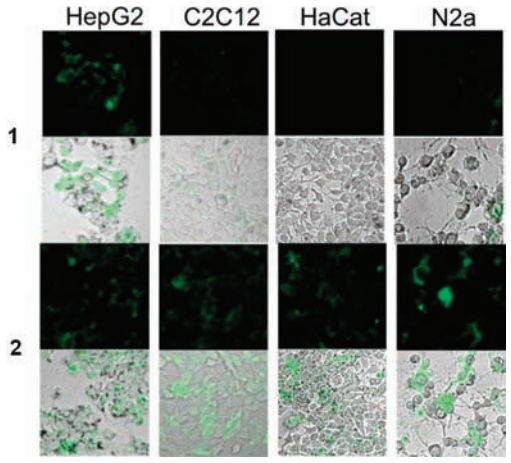

Figure 3. Confocal microscopy images of HepG2, C2C12, HaCat, and N2a cells treated with **1** (10 μM) and **2** (1.0 μM). The cells were incubated with media containing 10^{-8} M biotin for 2 days at 37 °C, washed, and incubated for 20 min with PBS solution containing **1** or **2**. The bottom panels show overlays of the fluorescence image with a nonconfocal phase contrast one. Cell images were obtained using an excitation wavelength of 458 nm and a band-path (530−600 nm) emission filter. Note that a lower concentration of **2** was used because it is taken up into cells in a nonspecific manner and gives a strong fluorescent image across all cell types subject to study.

(λ_{em} = 541 nm, Φ_f = 0.05) regardless of the cell type and does so in the presence and absence of biotin in the media. The use of biotin in these studies reflects the fact that the expression levels of the asialoglycoprotein receptor (ASGP-R) in HepG2 cells are generally low[20] but can be induced by biotin treatment.[21] Consistent with such literature reports and fully in accord with our design expectations, the fluorescence intensity of **1** in HepG2 cells was found to depend on the concentration of biotin in the cellular medium (Figure S20). Moreover, fluorescence changes were seen in the case of the other cell lines noted above. This behavior stands in marked contrast to what is seen in the case of **2** and is thus consistent with the proposed endocytosis uptake mechanism.

To obtain further support for the proposed endocytosis process, analogous cell uptake experiments were carried out in the presence of okadaic acid (Figure S21). This latter agent is known as an inhibitor of ASGP-R endocytosis,[22] and its effect is concentration dependent. We observed that the fluorescence changes of **1** in HepG2 cells were delayed in the presence of okadaic acid. On the basis of this experiment and those described above, we conclude that cellular uptake of **1** into HepG2 cells is indeed mediated via endocytosis. Interestingly, the fluorescence intensity of **1** (row A of Figure S23) increases faster than that of **2** (row B of Figure S23). Presumably, this reflects the fact that the disulfide bond cleavage of **1** can occur either in the cytosol after transfer from the endosome or within the endosome by an enzyme such as lysosomal thiol reductase.[23]

To determine whether the fluorescence changes seen with **1** and **2** resulted from the disulfide cleavage reaction shown in Figure 2c, the cells were treated with NEM (*N*-ethylmaleimide). NEM is known to react with thiol groups. Therefore, in the presence of this agent, the fluorescence of cells treated with **1** or **2** was expected to be relatively decreased. In fact, this proved to be the case (Figure S22), as would be expected for a scenario wherein the fluorescence emission intensity of **1** and **2** depends on the intracellular thiol levels. Thus, on the basis of the results shown in Figure 3 in conjunction with those in Figures S20−22, we conclude that probe **1** is taken up selectively into HepG2 cells through ASGP-R-mediated endocytosis and gives rise to a fluorescence signature (with the greatest intensity enhancement being seen at 540 nm) as the result of thiol-induced disulfide bond cleavage and production of free aminonaphthalimide. In other words, all available evidence is consistent with the mode of action proposed in Figure 2c.

To validate whether imaging of hepatocytes could be achieved with probe **1** in vivo, animal studies were carried out using Male Sprague−Dawley rats as our model. Here, probe **1** or **2** was administered at 1.5 and 0.8 mg/kg dose level, respectively, via tail-vein injection. 1.5 h postinjection, the rats were anesthetized and sacrificed by cervical dislocation. The organs were then quickly removed and washed with cold PBS buffer. To characterize the distribution of **1** and **2** in various organs, fluorescence images of various tissue sections (thickness 10 μm) were measured using confocal microscopy. A normal rat that was not subject to injection of either **1** or **2** was used as a control. Figure 4 shows the fluorescent images of **1** and **2** in several organs such as the liver, lungs, kidneys, pancreas, and heart. The images in question provide confirmation that **1** accumulates selectively in the liver (panel b), as reflected in observable fluorescent imaging, whereas little fluorescence was detected from other organs (panels e, h, k, and n). In contrast, significant accumulation in both liver (panel c) and kidney (panel i) was apparent in the case of **2**. This contrasting behavior is fully consistent with the proposition that probe **1**, but not the control system **2**, is taken up preferentially by liver tissue. On the basis of the in vitro studies detailed above, we infer that this occurs as the result of ASGP-R-mediated

dx.doi.org/10.1021/ja210065g | J. Am. Chem.Soc. 2012, 134, 1316−1322

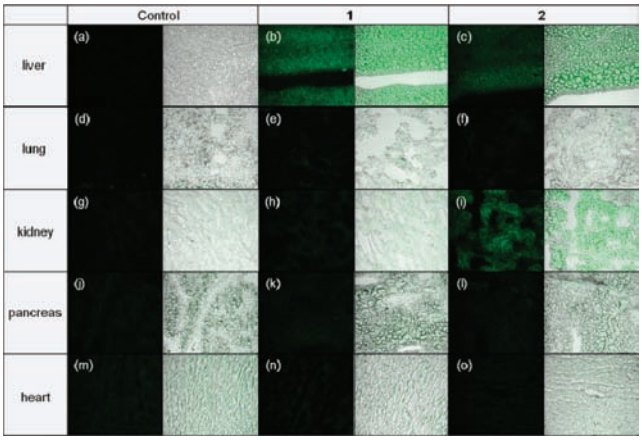

Figure 4. Confocal microscopy images of the tissue sections taken from a control rat and two rats that were injected with probes **1** and **2** (0.5 μmol in 500 μL of H_2O), respectively. Each panel shows the fluorescence image and an overlay of the fluorescence image with a phase contrast one. Cell images were obtained using an excitation wavelength of 458 nm and a band-path (530−600 nm) emission filter.

endocytosis and that, once taken up into liver cells, thiol-induced disulfide bond cleavage serves to convert probe **1** into its free amino fluorescent form. It could be also possible that the disulfide bond cleavage take places in part prior to liver targeting by the galactose unit in **1**. However, independent of mechanism, it is important to appreciate that this new probe shows great promise for organ specific targeting and imaging in vivo.

The ability of **1** to target into and then image free thiol levels in hepatocyte both in vitro and in vivo leads us to propose it could have utility in the area of drug candidate screening and as a marker for potential disease states. It is well-known that oxidative stress events induce a depletion of cellular thiol levels and that reduced thiol levels are correlated with pathogenic states.[24] As a preliminary test of this possibility, HepG2 cells were treated with palmitate (PA), a toxic saturated fatty acid.[25] The cells were incubated with and without PA (0.7 mM) for 24 h followed by addition of **1** (10 μM). Fluorescence images were then acquired by confocal microscopy. As can be seen by inspection of Figure 5, PA-treated HepG2 cells give rise to a weaker fluorescence response than control HepG2 cells that were not treated with this toxic agent. We thus believe that appropriately designed studies, wherein **1** is used as a probe, could be used to screen agents, including potential drug candidates, which mediate the effects of oxidative stress.

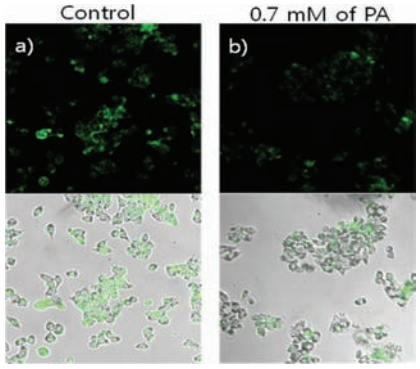

Figure 5. Confocal microscopy images of palmitate-induced lipotoxicity of HepG2 cell, a model of metabolic syndrome. The cells were incubated with media containing 10^{-8} M biotin for 2 days and with (a) or without (b) 0.7 mM palmitate (PA) for another 24 h at 37 °C, washed, and incubated for 20 min with PBS solution containing **1** (10 μM). Bottom panels show an overlay of the image with a phase contrast image. Cell images were obtained using an excitation wavelength of 458 nm and a band-path (530−600 nm) emission filter.

CONCLUSIONS

We have described the synthesis, characterization, spectroscopic properties, and biological applications of **1**, a new single galactose-appended naphthalimide. This system allows for the selective targeting of hepatocyte and gives rise to an enhanced fluorescence emission upon exposure to free thiols, both in vitro and in vivo. Compound **1** features good water solubility, an easy-to-visualize, analyte-dependent fluorescence response time, and little cross reactivity over a wide pH range. We thus think that this system may have a role to play in the in vitro and in vivo diagnostics, and in the screening of new potential drug agents. More broadly, we suggest that the strategy outlined herein could provide a powerful new approach for the construction of tissue-selective probes and for the generation of small molecule carrier agents that localize selectively to a given organ as the result of specifically exploited endocytosis mechanisms.

EXPERIMENTAL SECTION

The four naphthalimide derivatives **3a**, **3b**, **4a**, and **4b**[17,18] and the acetylated galactose amine, **AcGal-NH$_2$**,[19] were prepared in accord with procedures reported earlier.

Synthesis of 5. A mixture of **4a** (0.9 g, 3.1 mmol), EDCI (0.7 g, 3.1 mmol), and DMAP (0.8 g, 6.2 mmol) in anhydrous DMF was stirred under nitrogen for 10 min at room temperature. **AcGal-NH$_2$** (2.0 g, 3.1 mmol) was then added to the mixture. The reaction mixture was stirred overnight. The solvent was evaporated off, after which CH_2Cl_2 (100 mL) and water (100 mL) were added, and the organic layer was collected. The CH_2Cl_2 layer was dried with anhydrous $MgSO_4$. After removal of the solvents, the crude product was purified over silica gel using CH_2Cl_2/MeOH (v/v, 97:3) as the eluent to yield **5** as a yellowish oil (1.7 g, 72%). IR (sample deposited from a dichloromethane solution onto a NaCl plate, cm^{-1}): 3370, 3250, 2920, 2870, 1750, 1640, 1580. ESI−MS m/z (M^+) calcd 745.7, found 768.7 (M + Na^+). HRMS m/z calcd (M + H^+) 746.2772, found 746.2770. ^{1}H NMR ($CDCl_3$, 400 MHz): δ 8.45 (d, 1H, J = 7.2 Hz), 8.25−8.18 (m, 2H), 7.49 (t, 1H, J = 8.0 Hz), 6.76 (d, 1H, J = 8.2 Hz), 6.66 (t, 1H, J = 4.40 Hz), 5.80 (s, 2H), 5.40 (d, 1H, J = 3.3 Hz), 5.31−5.19 (m, 1H), 5.05−5.01 (m, 1H), 5.56 (d, 1H, J = 4.6 Hz), 4.47 (d, 2H, J = 7.2 Hz), 4.19−3.71 (m, 3H), 3.77−3.47 (m, 12H), 2.70 (t, 2H, J = 7.2 Hz), 2.13 (s, 3H), 2.07 (s, 3H), 2.04 (s, 3H), 2.00 (s, 3H). ^{13}C NMR ($CDCl_3$, 100 MHz): 171.3, 170.6, 169.8, 164.7, 164.0, 151.2, 134.2, 131.5, 129.9, 128.3, 122.4, 119.9, 110.1, 109.2, 101.5, 71.0, 70.8, 70.3, 69.8, 69.0, 67.3, 61.5, 39.5, 36.9, 35.3, 20.9 ppm.

Synthesis of 6. To a mixture of **5** (0.3 g, 0.4 mmol) and triphosgene (0.3 g, 0.8 mmol) in 20 mL of dry toluene was added DIPEA (0.3 mL, 1.4 mmol) dropwise. The resulting solution was heated at reflux for 3 h. After being cooled to room temperature, the reaction mixture was flushed with nitrogen gas. After removal of the unreacted phosgene gas (Caution: Toxic!) and neutralizing in an NaOH bath, a solution of 2,2′-dithiodiethanol (0.3 g, 2.0 mmol) in distilled CH_2Cl_2 (5 mL) was added to the mixture. The reaction mixture was stirred overnight. The solvent was evaporated off, at which point CH_2Cl_2 (100 mL) and water (100 mL) were added, and the organic layer was collected. The CH_2Cl_2 layer was dried using anhydrous $MgSO_4$. After removal of the solvents, the crude product was purified over silica gel using ethyl acetate/MeOH (v/v, 98:2) as the eluent to yield **6** as a yellowish oil (150.0 mg, 60%). IR (sample deposited from a dichloromethane solution onto a NaCl plate, cm^{-1}): 3342, 3250, 2919, 1650, 1538. ESI−MS m/z (M^+) calcd 925.3, found 924.4 (M − H^+). HRMS m/z (M + H^+) calcd 926.2687, found 926.2690.

dx.doi.org/10.1021/ja210065g | J. Am. Chem.Soc. 2012, 134, 1316−1322

^{1}H NMR ($CDCl_3$, 400 MHz): δ 8.55 (s, 1H), 8.39−8.28 (m, 3H), 8.11 (d, 1H, J = 8.2 Hz), 7.55 (t, 1H, J = 8.0 Hz), 6.79 (t, 1H, J = 4.40 Hz), 5.38 (d, 1H, J = 3.1 Hz), 5.22−5.17 (m, 1H), 5.03−4.99 (m, 1H), 4.56−4.50 (m, 3H), 4.41 (t, 2H, J = 7.1 Hz), 4.14−3.67 (m, 3H), 3.66−3.46 (m, 12H), 3.08 (t, 2H, J = 6.4 Hz), 2.96 (t, 2H, J = 6.0 Hz), 2.69 (t, 2H, J = 7.1 Hz), 2.14 (s, 3H), 2.06 (s, 3H), 2.03 (s, 3H), 1.97 (s, 3H). ^{13}C NMR ($CDCl_3$, 100 MHz): 171.2, 170.6, 169.8, 164.1, 163.6, 153.6, 139.9, 132.4, 131.3, 128.7, 127.5, 126.4, 123.2, 122.7, 117.2, 101.5, 71.0, 70.8, 70.3, 69.8, 69.0, 67.2, 64.0, 63.7, 61.5, 60.6, 41.8, 39.5, 37.7, 37.1, 34.8, 39.9, 20.8 ppm.

Synthesis of 2. To a mixture of **4b** (0.2 g, 0.7 mmol) and triphosgene (0.4 g, 1.4 mmol) in 20 mL of toluene was added DIPEA (0.5 mL, 2.5 mmol) dropwise. The resulting solution was refluxed for 3 h. After being cooled to room temperature, the reaction mixture was flushed with nitrogen gas. After removal of unreacted phosgene gas (Caution: Toxic!) and neutralizing in an NaOH bath, a solution of 2,2′-dithiodiethanol (0.6 g, 3.5 mmol) in CH_2Cl_2 (5 mL) was added to the mixture. The reaction mixture was stirred overnight. The solvent was evaporated off, at which point CH_2Cl_2 (100 mL) and water (100 mL) were added, and the organic layer was collected. The CH_2Cl_2 layer was dried over anhydrous $MgSO_4$. After removal of the solvents, the crude product was purified over silica gel using ethyl acetate/hexanes (v/v, 3:2) as the eluent to yield **2** as a yellow solid (200.0 mg, 60%). Mp 123−124 °C. IR (sample deposited from a dichloromethane solution onto a NaCl plate, cm^{-1}): 3430, 2910, 1640, 1360, 1260. ESI−MS m/z (M^+) calcd 448.1, found 447.1 ($M - H^+$). HRMS m/z ($M + H^+$) calcd 449.1205, found 449.1204. ^{1}H NMR ($CDCl_3$, 400 MHz): δ 8.62−8.56 (m, 2H), 8.34 (d, 1H, J = 8.2 Hz), 8.25 (d, 1H, J = 8.5 Hz), 7.82 (br, 1H), 7.75 (t, 1H, J = 8.0 Hz), 4.56 (t, 2H, J = 6.3 Hz), 4.16 (d, 2H, J = 7.5 Hz), 3.96 (t, 2H, J = 5.6 Hz), 3.06 (t, 2H, J = 6.3 Hz), 2.96 (t, 2H, J = 5.8 Hz), 2.42 (br, 1H), 1.74−1.67 (m, 2H), 1.47−1.39 (m, 2H), 0.97 (t, 3H, J = 7.3 Hz). ^{13}C NMR ($CDCl_3$, 100 MHz): 164.1, 163.6, 152.9, 138.8, 132.4, 131.2, 128.8, 126.6, 126.1, 123.3, 123.0, 117.9, 116.9, 63.8, 60.5, 41.5, 40.2, 37.4, 30.2, 20.4, 13.8 ppm.

Synthesis of 1. To a solution of **6** (60.0 mg, 0.06 mmol) in MeOH (2 mL) was added sodium methoxide (129 μL from a 0.5 M solution in MeOH). The reaction mixture was stirred at room temperature until the starting material disappeared (as evidenced by TLC analysis). The solution was neutralized via the addition of a cation-exchange resin (H^+), filtered, and washed with MeOH. The solvent was then removed in vacuo. The solid obtained in this way was recrystallized from DCM to afford **1** as a yellow solid (30.0 mg, 61%). Mp 109−110 °C. IR (sample deposited from a dichloromethane solution onto a NaCl plate, cm^{-1}): 3340, 2920, 1650, 1540. ESI−MS m/z (M^+) calcd 757.2, found 756.3 ($M - H^+$). HRMS m/z ($M + H^+$) calcd 758.2265, found 758.2267. ^{1}H NMR (CD_3OD, 400 MHz): δ 8.56−8.49 (m, 3H), 8.22 (d, 1H, J = 8.2 Hz), 7.81−7.78 (m, 1H), 4.51 (t, 2H, J = 6.4 Hz), 4.41 (t, 2H, J = 7.0 Hz), 4.18 (d, 1H, J = 7.5 Hz), 3.95−3.30 (m, 20H), 3.08 (t, 2H, J = 6.5 Hz), 2.88 (t, 2H, J = 6.7 Hz), 2.60 (t, 2H, J = 7.0 Hz). ^{13}C NMR ($CDCl_3$, 100 MHz): 173.8, 165.6, 165.0, 155.8, 142.2, 133.1, 132.4, 130.0, 129.9, 127.6, 125.7, 124.0, 119.5, 118.9, 105.1, 76.7, 74.8, 72.5, 71.3, 71.0, 70.5, 70.2, 69.4, 64.7, 62.5, 61.2, 42.2, 40.4, 38.3, 38.1, 35.7 ppm.

Spectroscopic Materials and Methods. Stock solutions of biologically relevant analytes [thiols, Val, Tyr, Thr, Tau, Ser, Pro, Phe, Met, Lys, Leu, Ile, His, Gly, Gluc, Glu, Gln, Asp, Asn, Arg, Ala, Zn(II), Na(I), Mg(II), K(I), Fe(III), Fe(II), Cu(II), and Ca(II)] were prepared in triple distilled water. A stock solution of **1** was also prepared in triple distilled water. All spectroscopic measurements were performed under physiological conditions (PBS buffer, pH 7.4, 37 °C). The fluorescence quantum yield (Φ_f) was measured relative to quinine (Φ_f = 0.54 in 0.5 M H_2SO_4).[26] Absorption spectra were recorded on an S-3100 (Scinco) spectrophotometer, and fluorescence spectra were recorded using an RF-5301 PC spectrofluorometer (Shimadzu) equipped with a xenon lamp. Samples for absorption and emission measurements were contained in quartz cuvettes (3 mL volume). Excitation was provided at 428 nm with excitation and emission slit widths of 3 and 5 nm, respectively.

Preparation of Cell Cultures. HepG2 (human hepatoma), C2C12 (mouse myoblast), HaCat (human keratinocyte), and N2a (mouse neuroblastoma) cell lines were used in this study. Each cell line was cultured in Dulbecco's Modified Eagle Medium (DMEM) supplemented with 10% fetal bovine serum, 1% penicillin−streptomycin at 37 °C under humidified air containing 5% CO_2. 1×10^5 of the cells were seeded on 24-well plates and stabilized overnight and achieved confluence in 2 days in DMEM containing 10^{-8} M biotin for expression of the asialoglycoprotein receptor (ASGP-R). Compound **1** was applied to the cell to detect cellular thiols as discussed in the main text. In some experiments, the cells were incubated with media containing NEM, okadaic acid, or palmitate prior to treatment with **1**. Next, the cells were briefly washed with 1 mL of PBS and were then treated with **1** (10 μM) in PBS. After 20 min incubation, the remaining **1** in the PBS was removed by washing three times with PBS, and the cells were placed in 1 mL of PBS solution. The fluorescence images were taken with a 200 × 4 objective using a confocal laser scanning microscope (Zeiss LSM 510, Zeiss, Oberko, Germany) that was equipped with a 458 nm argon laser and a band-pass (530−600 nm) emission filter.

Animal Experiments. Male Sprague−Dawley rats were purchased from Orient Bio Experimental Animal Center (Samtako, Korea). All animals were acclimatized to the animal facility for at least 48 h prior to experimentation. The rats were kept in a barrier under HEPA filtration and in a 12 h/12 h light/dark cycle, and given food and water ad libitum. Each rat weighed 200−250 g. 0.5 μmol/500 μL of **1** (1.5 mg/kg) and **2** (0.8 mg/kg) were administered to the rats via tail-vein injection, respectively. A freshly dissected tissue block (<5 mm thick) was placed onto a prelabeled tissue base mold and covered with cryo-embedding media (optimal cutting temperature compound). Each tissue block was submerged in liquid nitrogen to ensure the tissue is completely frozen. The frozen tissue block was stored at −80 °C until ready for sectioning, and then the frozen tissue block was transferred to a cryotome cryostat (−20 °C) prior to sectioning. Subsequently, the blocks were cut with the microtome portion of the cryostat. Each section (thickness 10 μm) was picked up on a glass slide for analysis by confocal fluorescent microscopy. All animal experimental procedures were approved by the local ethical committee for animal experiments. Animals were treated humanely with regard to alleviation of suffering.

■ ASSOCIATED CONTENT

Supporting Information

Additional spectra (UV/vis absorption, fluorescence, NMR, ESI−MS) and imaging data and full reference information. This material is available free of charge via the Internet at http://pubs.acs.org.

■ AUTHOR INFORMATION

Corresponding Author

kangch@khu.ac.kr; jongskim@korea.ac.kr

■ ACKNOWLEDGMENTS

This work was supported by the CRI project (2011-0000420) of the National Research Foundation of Korea. J.L.S. would like to thank the WCU (World Class University) program (R32-2010-000-10217-0) administered through the National Research Foundation of Korea funded by the Ministry of Education, Science, and Technology (MEST).

■ REFERENCES

(1) (a) Smilkstein, M.; Sriwilaijaroen, N.; Kelly, J. X.; Wilairat, P.; Riscoe, M. *Antimicrob. Agents Chemother.* **2004**, *48*, 1803−1806. (b) Seethala, R., Fernandes, R. B., Dekker, M., Eds. *Handbook of Drug Screening*; Drugs and the Pharmaceutical Sciences: New York, 2001. (c) Hargrove, A. E.; Nieto, S.; Zhang, T.; Sessler, J. L.; Anslyn, E. V. *Chem. Rev.* **2011**, *111*, 6603−6782.

(2) (a) Lakowicz, L. R. *Principles of Fluorescence Spectroscopy*; Springer: New York, 2011. (b) Tsien, R. Y. In *Fluorescent and Photochemical Probes of Dynamic Biochemical Signals Inside Living Cells*; Czarnik, A. W., Ed.; American Chemical Society: Washington, DC, 1993; pp 130−146. (c) Mason, W. T. *Fluorescent and Luminescent Probes for Biological Activity*, 2nd ed.; Academic Press: New York, 1999. (d) Nagano, T.; Yoshimura, T. *Chem. Rev.* **2002**, *102*, 1235−1270. (e) Que, E. L.; Domaille, D. W.; Chang, C. J. *Chem. Rev.* **2008**, *108*, 1517−1549.

(3) (a) Lu, S. C. *Curr. Top. Cell. Regul.* **2000**, *36*, 95−116. (b) Dalton, T. P.; Shertzer, H. G.; Puga, A. *Annu. Rev. Pharmacol. Toxicol.* **1999**, *39*, 67−101. (c) Deneke, S. M.; Fanburg, B. L. *Am. J. Physiol.* **1989**, *257*, L163−L173.

(4) (a) Akerboom, T. P.; Bilzer, M.; Sies, H. *J. Biol. Chem.* **1982**, *257*, 4248−4252. (b) Griffith, O. W. *Free Radical Biol. Med.* **1999**, *27*, 922−935. (c) Townsend, D. M.; Tew, K. D.; Tapiero, H. *Biomed. Pharmacother.* **2003**, *57*, 145−155. (d) Han, D.; Hanawa, N.; Saberi, B.; Kaplowitz, N. *Am. J. Physiol.* **2006**, *291*, G1−G7. (e) Ścibior, D.; Skrzycki, M.; Podsiad, M.; Czeczot, H. *Clin. Biochem.* **2008**, *41*, 852−858.

(5) (a) Sessler, J. L.; Miller, R. A. *Biochem. Pharmacol.* **2000**, *59*, 733−739. (b) Magda, D.; Lepp, C.; Gerasimchuk, N.; Lee, I.; Sessler, J. L.; Lin, A.; Biaglow, J.; Miller, R. A. *Int. J. Radiat. Oncol., Biol., Phys.* **2001**, *51*, 1025−1036. (c) Magda, D. J.; Sessler, J. L.; Gerasimchuk, N.; Miller, R. A. In *Med. Inorg. Chem.*; Sessler, J. L., Doctrow, S., McMurry, T., Lippard, S. J., Eds.; American Chemical Society Symposium Series; Oxford University Press: New York, 2005.

(6) (a) Pullela, P. K.; Chiku, T.; Carvan, M. J.; Sem, D. S. *Anal. Biochem.* **2006**, *352*, 265−273. (b) Shao, N.; Jin, J.; Wang, H.; Zheng, J.; Yang, R.; Chan, W.; Abliz, Z. *J. Am. Chem. Soc.* **2010**, *132*, 725−736. (c) Chen, X.; Zhou, Y.; Peng, X.; Yoon, J. *Chem. Soc. Rev.* **2010**, *39*, 2120−2135. (d) Yin, L.-L.; Chen, Z.-Z.; Tong, L.-L.; Xu, K.-H.; Tang, B. *Chin. J. Anal. Chem.* **2009**, *37*, 1073−1081. (e) Jung, H. S.; Ko, K. C.; Kim, G. H.; Lee, A. R.; Na, Y. C.; Kang, C.; Lee, J. Y.; Kim, J. S. *Org. Lett.* **2011**, *13*, 1498−1501. (f) Jung, H. S.; Han, J. H.; Habata, Y.; Kang, C.; Kim, J. S. *Chem. Commun.* **2011**, *47*, 5142−5144. (g) Lim, C. S.; Masanta, G.; Kim, H. J.; Han, J. H.; Kim, H. M.; Cho, B. R. *J. Am. Chem. Soc.* **2011**, *133*, 11132−11135.

(7) Kaplowitz, N. *Yale J. Biol. Med.* **1981**, *54*, 497−502.

(8) (a) Obrador, E.; Benlloch, M.; Pellicer, J. A.; Asensi, M.; Estrela, J. M. *J. Biol. Chem.* **2011**, *286*, 15716−15727. (b) Kaplowitz, N.; Aw, T. Y.; Ookhtens, M. *Annu. Rev. Pharmacol. Toxicol.* **1985**, *25*, 715−744.

(9) (a) Mahato, R.; Tai, W.; Cheng, K. *Adv. Drug Delivery Rev.* **2011**, *63*, 659−670. (b) Wu, J.; Nantz, M. H.; Zern, M. A. *Front. Biosci.* **2002**, *7*, d717−d725.

(10) (a) Ashwell, G.; Harford, J. *Annu. Rev. Biochem.* **1982**, *51*, 531−554. (b) Spiess, M. *Biochemistry* **1990**, *29*, 10009−10018.

(11) (a) Wu, G. Y.; Wu, C. H. *Adv. Drug Delivery Rev.* **1998**, *29*, 243−248. (b) Yamazaki, N.; Kojima, S.; Bovin, N. V.; André, S.; Gabius, S.; Gabius, H.-J. *Adv. Drug Delivery Rev.* **2000**, *43*, 225−244. (c) Cai, G.; Jiang, M.; Zhang, B.; Zhou, Y.; Zhang, L.; Lei, J.; Gu, X.; Cao, G.; Jin, J.; Zhang, R. *Biol. Pharm. Bull.* **2009**, *32*, 440−443. (d) Yang, W.; Mou, T.; Peng, C.; Wu, Z.; Zhang, X.; Li, F.; Ma, Y. *Bioorg. Med. Chem.* **2009**, *17*, 7510−7516.

(12) (a) Lee, R. T.; Lin, P.; Lee, Y. C. *Biochemistry* **1984**, *23*, 4255−4261. (b) Managit, C.; Kawakami, S.; Yamashita, F.; Hashida, M. *Int. J. Pharm.* **2005**, *301*, 255−261. (c) Kallinteri, P.; Papadimitriou, E.; Antimisiaris, S. G. *J. Liposome Res.* **2001**, *11*, 175−193. (d) Van Berkel, T. J. C.; Kruijt, J. K.; Spanjer, H. H.; Nagelkerke, J. F.; Harkes, L.; Kempen, H.-J. M. *J. Biol. Chem.* **1985**, *260*, 2694−2699. (e) Huang, A.; Huang, L.; Kennel, S. J. *J. Biol. Chem.* **1980**, *255*, 8015−8018.

(13) (a) Sliedregt, L. A. J. M.; Rensen, P. C. N.; Rump, E. T.; Van Santbrink, P. J.; Bijsterbosch, M. K.; Valentijn, A. R. P. M; Van der Marel, G. A.; Van Boom, J. H.; Van Berkel, T. J. C.; Biessen, E. A. L. *J. Med. Chem.* **1999**, *42*, 609−618. (b) Rensen, P. C. N.; Schiffelers, R. M.; Versluis, A. J.; Bijsterbosch, M. K.; Van Kuijk-Meuwissen, M. E. M. J.; Van Berkel, T. J. C. *Mol. Pharmacol.* **1997**, *52*, 445−455.

(14) (a) Yang, W.; Mou, T.; Guo, W.; Jing, H.; Peng, C.; Zhang, X.; Ma, Y.; Liu, B. *Biol. Med. Chem. Lett.* **2010**, *20*, 4840−4844. (b) Kim, E.-M.; Jeong, H.-J.; Kim, S.-L.; Sohn, M.-H.; Nah, J.-W.; Bom, H.-S.; Park, I.-K.; Cho, C.-S. *Nucl. Med. Biol.* **2006**, *33*, 529−534. (c) Kim, E.-M.; Jeong, H.-J.; Park, I.-K.; Cho, C.-S.; Moon, H.-B.; Yu, D.-Y.; Bom, H.-S.; Sohn, M.-H.; Oh, I.-J. *J. Controlled Release* **2005**, *108*, 557−567.

(15) (a) Lee, Y. C.; Townsend, R. R.; Hardy, M. R.; Lonngren, J.; Arnarp, J.; Haraldsson, M.; Lonn, H. *J. Biol. Chem.* **1983**, *258*, 199−202. (b) Lee, Y. C.; Lee, R. T. *Acc. Chem. Res.* **1995**, *28*, 321−327.

(16) (a) Zhang, J. F.; Lim, C. S.; Bhuniya, S.; Cho, B. R.; Kim, J. S. *Org. Lett.* **2011**, *13*, 1190−1193. (b) Srikun, D.; Miller, E. W.; Domaille, D. W.; Chang, C. J. *J. Am. Chem. Soc.* **2008**, *130*, 4596−4597.

(17) Patrick, L. G. F.; Whiting, A. *Dyes Pigm.* **2002**, *55*, 123−132.

(18) Yuan, D.; Brown, R. G.; Hepworth, J. D.; Alexiou, M. S.; Tyman, J. H. P. *J. Heterocycl. Chem.* **2008**, *45*, 397−404.

(19) Sato, H.; Hayashi, E.; Yamada, N.; Yatagai, M.; Takahara, Y. *Bioconjugate Chem.* **2001**, *12*, 701−710.

(20) Pujol, A. M.; Cuillel, M.; Renaudet, O.; Lebrun, C.; Charbonnier, P.; Cassio, D.; Gateau, C.; Dumy, P.; Mintz, E.; Delangle, P. *J. Am. Chem. Soc.* **2011**, *133*, 286−296.

(21) Collins, J. C.; Paiettall, E.; Green, R.; Morell, A. G.; Stockert, R. J. *J. Biol. Chem.* **1988**, *263*, 11280−11283.

(22) Holen, I.; Gordon, P. B.; Stromhaug, P. E.; Berg, T. O.; Fengsrud, M.; Brech, A.; Roos, N.; Bergs, T.; Seglen, P. O. *Biochem. J.* **1995**, *311*, 317−326.

(23) Arunachalam, B.; Phan, U. T.; Geuze, H. J.; Cresswell, P. *Proc. Natl. Acad. Sci. U.S.A.* **2000**, *97*, 745−750.

(24) (a) Finkel, T.; Serrano, M.; Blasco, M. A. *Nature* **2007**, *448*, 767−774. (b) Rossi, D. J.; Jamieson, C. H. M.; Weissman, I. L. *Cell* **2008**, *132*, 681−696. (c) Houstis, N.; Rosen, E. D.; Lander, E. S. *Nature* **2006**, *440*, 944−948. (d) Barnham, K. J.; Masters, C. L.; Bush, A. I. *Nat. Rev. Drug Discovery* **2004**, *3*, 205−214.

(25) Das, S. K.; Mondal, A. K.; Elbein, S. C. *J. Lipid Res.* **2010**, *51*, 2121−2131.

(26) Crosby, G. A.; Demas, J. N. *J. Phys. Chem.* **1971**, *75*, 991−1024.